SGP-TR-145-2

PROCEEDINGS

EIGHTEENTH WORKSHOP GEOTHERMAL RESERVOIR ENGINEERING

January 26-28, 1993

Henry J. Ramey, Jr., Roland N. Horne,
Paul Kruger, Frank G. Miller,
William E. Brigham, Jean W. Cook
Stanford Geothermal Program
Workshop Report SGP-TR-145

DISCLAIMER

PROCEEDINGS, Eighteenth Workshop on Geothermal Reservoir Engineering
Stanford University, Stanford, California, January 26-28, 1993
SGP-TR-145

BULALO FIELD, PHILIPPINES: RESERVOIR MODELING FOR PREDICTION OF LIMITS TO SUSTAINABLE GENERATION

Calvin J. Strobel

Unocal Geothermal Division,
3576 Unocal Place, Santa Rosa, California, 95403-1774

ABSTRACT

The Bulalo geothermal field, located in Laguna province, Philippines, supplies 12% of the electricity on the island of Luzon. The first 110 MWe power plant was on line May 1979; current 330 MWe (gross) installed capacity was reached in 1984. Since then, the field has operated at an average plant factor of 76%. The National Power Corporation plans to add 40 MWe base load and 40 MWe standby in 1995.

A numerical simulation model for the Bulalo field has been created that matches historic pressure changes, enthalpy and steam flash trends and cumulative steam production. Gravity modeling provided independent verification of mass balances and time rate of change of liquid desaturation in the rock matrix. Gravity modeling, in conjunction with reservoir simulation provides a means of predicting matrix dry out and the time to limiting conditions for sustainable levelized steam deliverability and power generation.

INTRODUCTION

Bulalo field development, operations history, geology and geochemistry has been documented by Benavidez, et. al. (1988). Steam deliverability decline in individual wells has been moderate, 3-1/2% per year on average. Beginning in 1989 production makeup wells were needed to offset declines in steam deliverability to maintain peak power generation capacity. All produced brine has been injected since the beginning of production operations.

Conceptual modeling of the Bulalo field was initiated by the author in 1981. During the period 1981 to early 1983, injection flowmeter profiles were run in twenty four wells. A well by well analysis of temperature and pressure gradient profiles, geological data and enthalpy test data was accomplished using methods developed in New Zealand (Grant, Donaldson and Bixley, 1982). By early 1983 conceptual modeling had led to a general description of the resource: 1) thermodynamic state is distributed vapor to a depth of 5000 ft (1.5 km) bsl, with rising production enthalpy due to increasing vapor saturation, 2) the interconnected network of naturally enhanced permeability increased in area and volume with depth, 3) closed acting boundaries, depletion being from matrix desaturation and recirculation of injectate, and 4) mass in place within the network sufficient to sustain 330 MWe for 30 years at then prevailing evaporation rates.

The conceptual understanding as of 1983 has required little revision after 10 years of additional history and two reservoir simulation studies, except to change from notions of a closed system to one with significant influx. Simulation studies based upon field history through 1986, Atkinson and Pedersen (1988), had modeled the reservoir as a predominantly closed system with pressure support from brine injection. Enthalpy and pressure trends observed since 1986 can not be replicated with a closed system model. The current simulation effort described in this paper demonstrates that influx from above the reservoir, and from the northwest outside of the productive limits of the field is needed to match observed enthalpy and pressure trends and to provide the kind of mass balances necessary to match gravity changes.

THE SIMULATION MODEL

Model configuration and parameter assignments were the combined result of three interdependent processes: 1) conceptual modeling, 2) initial state simulation to reproduce known thermodynamic conditions and the dynamic pressure gradient in the reservoir and to match the initial enthalpy test values of production wells, and 3) history matching simulations to reproduce the trends of various dependent variables measured in the field to include

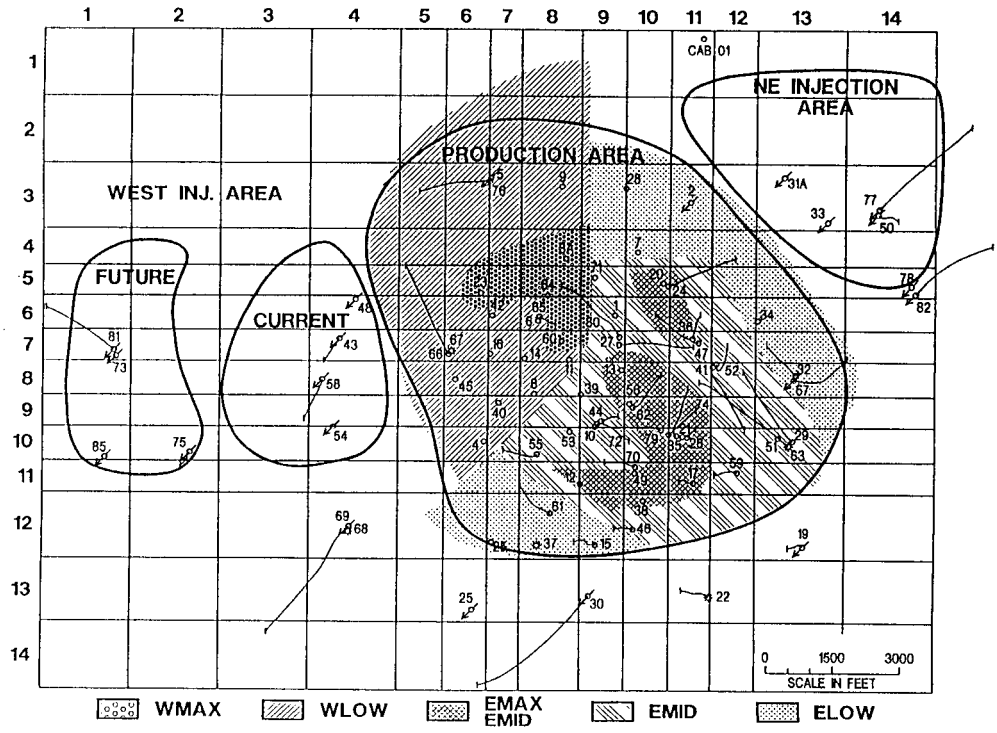

Fig. 1. Geographic distribution of the five enthalpy groups, and the injection strategy as of 1989.

enthalpy trends, pressure trends, cumulative steam production and steam flash (fraction of total mass that is vapor).

To perform the history matching simulations, the actual total mass production and injection histories of each well were imposed on the model. Independent variables discussed in the following sections of this paper were adjusted until the simulation model reproduced known trends and absolute values of the dependent variables.

Gridding and Well Completions

The numerical model has three layers of 196 rectangular blocks each arranged in 14 rows north-south and 14 columns east-west, as shown in Fig. 1. Each physical block is represented mathematically in the numerical model by a fracture block and a matrix block, the whole fracture matrix model being 1760 mathematical blocks.

Fig. 1 shows geographic dimensions of the grid relative to will locations. Total area of the grid is 20,000 feet (6098 m) east-west and 15,000 feet (4573 m) north-south, an area 6887 acres (2787 ha). Grid block size varies from 12 acres (4.86 ha) in the center, to 72 acres (29.1 ha) on the southeast and northwest.

Physically, the top layer represents depth from mean sea level to 1950 feet (595 m) bsl, the middle layer 1950 feet to 4650 feet (595 m to 1418 m) bsl, and the deepest layer 4650 to 7700 feet (1418 m to 2348 m) bsl. These depth intervals are shown in relation to well completion depths along a southwest to northeast cross section, Fig. 2. Injection wells are completed only in layers 2 and/or 3, compare depth intervals (Fig. 2) with injection areas (Fig. 1). Each production well is given layer assignments consistent with known well completion depth and enthalpy history matching results.

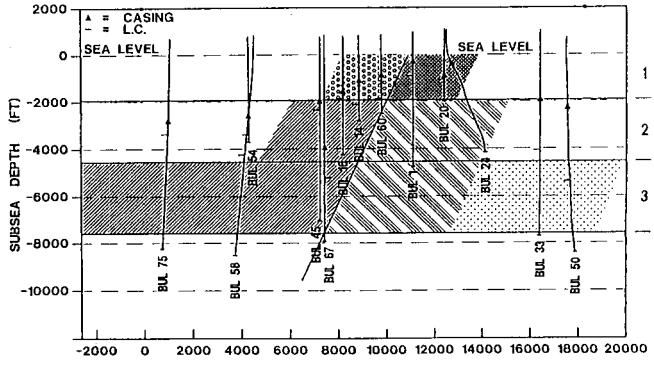

Fig. 2. Southwest - northeast cross section showing relation to the enthalpy groups.

Permeability and Porosity

Fracture and matrix permeability and porosity in the simulation model are summarized on Table 1. Matrix properties were assigned to the model beginning with average properties from core analysis and changing these properties in the model as necessary during the history matching process.

Some of the disparity between model properties and core data exists because cores are taken from specific points, whereas the simulation model requires an average value for the entire geographic area of each grid block. Also removal of the core from the natural hydrothermal environment to laboratory conditions may alter the original pore geometry and transmissibility.

Table 1. Porosity and Permeability

Layer	Model properties kxy,md.	Model properties ϕ,%	Core analysis averages number	Core analysis averages k,md.	Core analysis averages ϕ,%
1 fractures	100	.1	-	-	-
2 fractures	7.5-50	.1	-	-	-
3 fractures	7.5-25	.1	-	-	-
1 matrix	.03	12.5	4	.04	7.1
2 matrix	.03	7.5-9.0	18	.27	14.9
3 matrix	.03-.0045	5.5	18	.37	8.3

Reservoir Thermodynamics

At initial conditions vertical pressure gradient in the reservoir, interpreted from entry point conditions in the wells, exceeded hydrostatic by 10%. The excess gradient is a function of dynamic upward convection within the system, Grant, et. al. (1982 pp 162-165). To reproduce this pressure gradient in the simulation model, vertical permeability and aquifer influence were adjusted until the pressure gradient in the simulation model was the same as observed in the field data; this required low vertical permeability (.5 to 15 md.).

Rock temperatures in the model were set to maintain consistency with known entry point temperatures of the individual wells. At initial reservoir conditions many of the entry point temperatures and pressures were on the vapor pressure curve to a depth of 4650 feet (1418 m) bsl. A finite vapor saturation at initial conditions was necessary to match the beginning enthalpy behaviors of wells in the WMAX, EMAX and EMID enthalpy groups, Figs. 3 and 4. Initial vapor saturations, and therefore initial enthalpy test values, were very sensitive to rock temperature in the well completion blocks. Slight adjustments in grid block average temperatures were necessary to fine tune these initial state vapor saturation conditions.

In the interval from sea level to 1950 feet (595 m) bsl, average initial vapor saturations after initialization simulations were 30% for fracture blocks, and slightly less than 20% for the matrix blocks. Below 1950 feet (595 m) bsl there was no free vapor on the west side of the central barrier. East of the barrier in the interval from 1950 to 4650 feet (595 m to 1418 m) bsl, average initial vapor saturation in fractures was 20% and 7% in the rock matrix. No vapor phase existed below 4650 feet (1418 m) bsl.

Enthalpy and Pressure Trends

Five distinct production enthalpy patterns have been identified in the field, Figs. 3 and 4. Areal relationship of wells exhibiting a particular pattern is shown on Fig. 1 and vertical relationships are shown on Fig. 2.

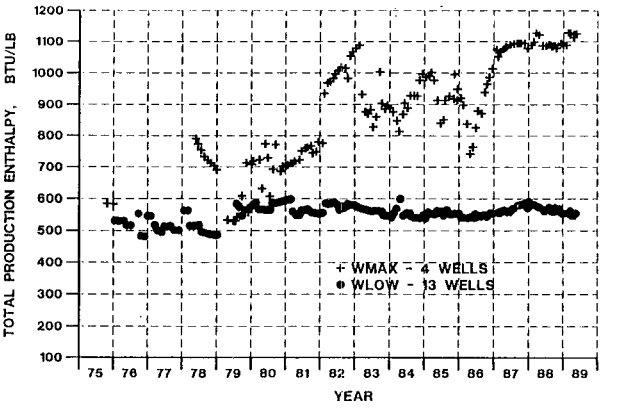

Fig. 3. West Bulalo enthalpy.

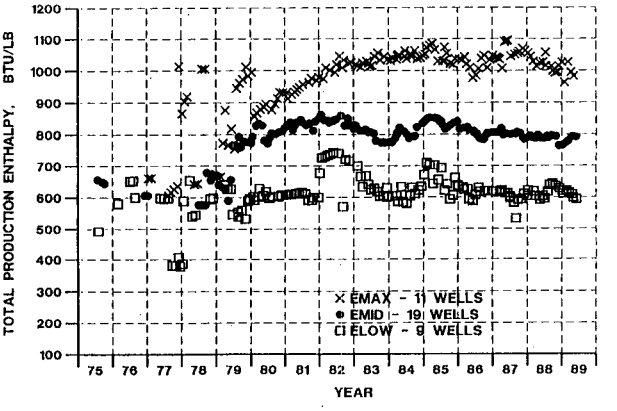

Fig. 4. East Bulalo enthalpy.

Table 2 shows the number of wells included in each group and approximate split of steam deliverability by group and by layer of the model. Although each well is represented individually in the simulation model, wells with similar enthalpy patterns appear to be influenced in unison by gross reservoir structural characteristics that the wells share in common.

Table 2. Percent of Total Steam Deliverability by Group and by Layer.

Group - Wells	Lyr-1	Lyr-2	Lyr-3	Total
WMAX -- 4	10	0	0	10
WLOW -- 16	2	10	3	15
EMAX -- 11	23	0	0	23
EMID -- 23	5	30	10	45
ELOW -- 11	1	3	3	7
TOTAL %	41	43	16	100

Comparison of group allocation percentages on Table 2 with the group enthalpy trends on Figs. 3 and 4 shows a relationship between observed enthalpy changes and well completion depth. On the west side of the reservoir the WMAX group, with all of its steam from layer 1, has rapidly rising enthalpy to 1000 Btu/lb (2326 KJ/kg) whereas the deeper WLOW group, with most of its steam from layer 2, has a very flat trend cycling between 550 and 600 btu/lb (1279 and 1395 KJ/kg). On the east side of the reservoir the EMAX group, with all of its steam from layer 1, has rapidly rising enthalpy to 1150 Btu/lb (2674 KJ/kg), compared to EMID group enthalpy which rises to 850 btu/lb (1977 KJ/kg) then begins gradual decline, and ELOW group enthalpy which has remained flat at 600 Btu/lb (1395 KJ/kg).

Layer 2 of the model, Fig. 2, is the primary production source, Table 2, for wells in the WLOW and EMID groups. Wells in these two groups are at equivalent completion depths, however there is a dramatic enthalpy discontinuity, compare Figs. 3 and 4, caused by the central barrier seen in Fig. 2. Influx from the northwest is held up by the barrier, isolating the east side. The result is higher enthalpy and greater pressure drawdown (Fig. 5) on the east.

History matching to enthalpy, Figs. 3 and 4, and the 500 psi (3.45 MPa) pressure sink on the southeast side of the field, Fig. 5, required a sensitive combination of influences, to include vertical transmissibility barriers, rate of downflux, mass flux across the central barrier, matrix permeability and relative permeability to steam and water in the matrix. The general shape and magnitude of enthalpy trends of the five groups shown on Figs. 3 and 4 were matched successfully, leading to the excellent matches to fieldwide flash trend, Fig. 6, and fieldwide cumulative steam produced, Fig. 7.

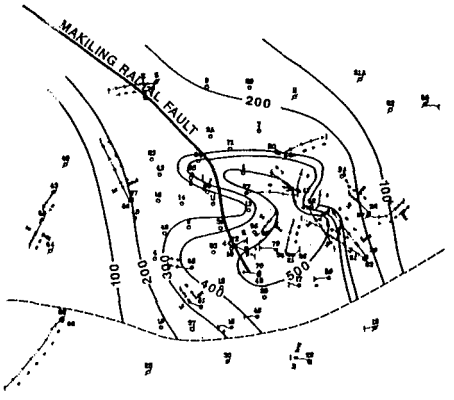

Fig. 5. Pressure drawdown, psi, from field data as of 1/1988.

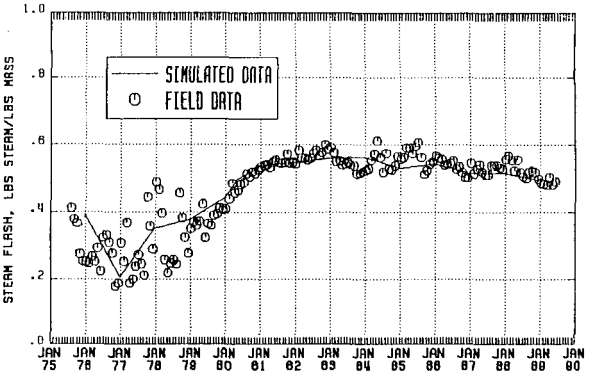

Fig. 6. Bulalo field total steam flash history match.

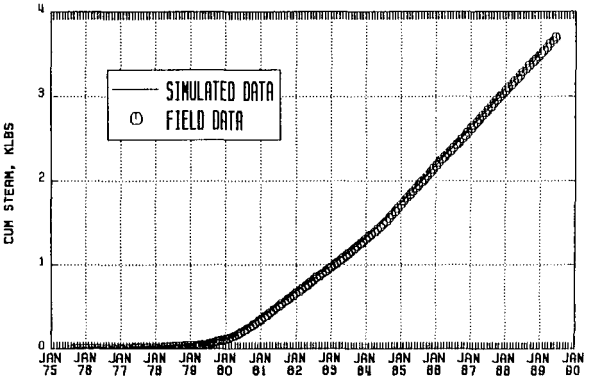

Fig. 7. Bulalo field cumulative steam history match.

At 80% vapor saturation in the fractures, relative permeability to vapor reaches 100%; liquid becomes immobile at 70% vapor saturation. At 80% vapor saturation in the matrix, water in the matrix becomes immobile and relative permeability to vapor reaches 100%. In Fig. 6, the maxima in 1983, and subsequent long term decline in fieldwide flash is due to downflux from above and within the reservoir. In 1983, pressure at the base of the caprock dropped below aquifer pressure reversing the convection path from outflow to inflow.

General shape and magnitude of the pressure sink shown on Fig. 5 was matched. Symmetric arrangement of pressure contours along the northwest trending Makiling Radial Fault indicates extension of high permeability reservoir to the northwest. Influx from the northwest provides pressure support west of the central barrier shown on Fig 2. A 500 psi (3.45 MPa) pressure sink exists east of the barrier. Matching this sink required another permeability barrier to the north between the eastern production area and the northeast injection area, Fig. 1, effectively isolating the eastern side of the field from active pressure support.

PREDICTIVE MODELING

Depletion Mechanisms

Reservoir simulation shows that pro-produced fluid mass originates from three sources currently acting in roughly equal proportions: (1) recovery of injected brine, (2) vaporization of liquid in matrix , and (3) influx from outside the boundaries of the model. Percentage of total mass production rate from each of these sources is shown on Table 3.

Table 3. Depletion Source, Percent of Total Mass Production Rate vs. Time.

Depletion source	1991	2011	2050
Matrix desaturation	33	14	3
Injected brine	37	30	36
Natural influx	30	56	61
Total mass rate	100	100	100

Vaporization of liquid in the rock matrix will become less important with time, influx will become more important and recovery of injected brine will remain fairly constant at approximately 1/3 of the total mass produced. The importance of injectate recirculation is confirmed by tracer testing, Villadolid (1991), which demonstrated widespread and rapid migration of injectate in the reservoir; in the simulation model, fracture/matrix geometry and heat transfer properties qualitatively reproduce the migration phenomena observed by Villadolid. Natural mass influx rate and cumulative were quantified by history matching to observed pressure and enthalpy changes. These influx numbers agreed quantitatively with those determined independently by modeling gravity changes, San Andres and Pedersen (1992).

Sustainable Limits

Predictive simulation incorporated addition of one 55 MWe unit to be operated at 76 % plant factor. This is equivalent to the expected average steam demand of the proposed plan to add 40 MWe base and 40 MWe standby.

Predictive modeling results, Fig. 8, show that by drilling infield production make up wells, existing generation levels (status quo) can be sustained until the year 2011, followed by declining generation. The proposed additions in 1995 (40 MWe base and 40MWe standby) are sustainable to the year 2005; this short term increase being offset by a corresponding long term decrease in power generation. Each of the two cases on Fig. 8 assumes the same limiting number of make up well locations.

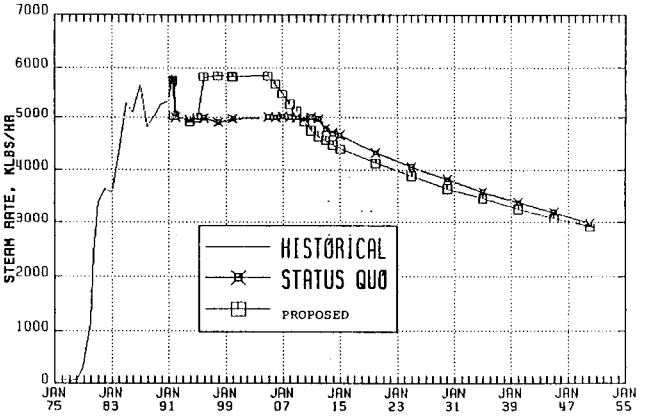

Fig. 8. Bulalo field total steam rate prediction showing the affect of proposed additions to capacity.

Gravity Modeling For Prediction of Matrix Dryout and Limits to Sustainable Deliverability

Observed gravity, San Andres and Pedersen (1992), verified the mass balances of the current reservoir simulation model, Fig. 9. The "1990" trend matches the OBSERVED GRAVITY very well. Difference between the PROD-INJ trend and the "1990" trend is due to influx of liquid. The OBSERVED GRAVITY trend is primarily due to saturation changes as vapor replaces liquid.

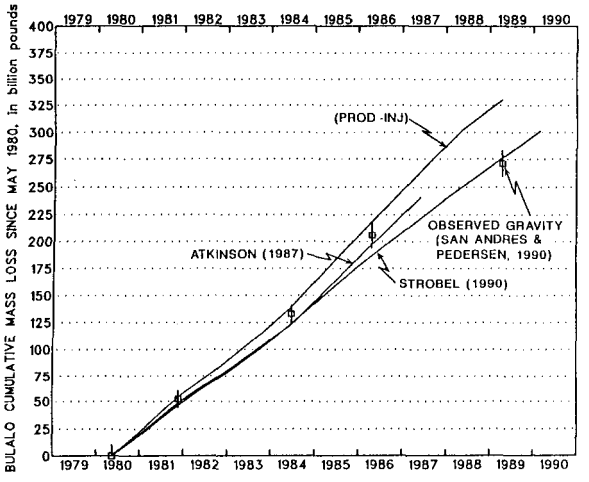

Fig. 9. Cumulative mass loss from observed gravity compared to actual voidage (PROD-INJ) and the simulations in 1987 (closed model) and 1990 (model with influx)

Reservoir simulation in conjunction with gravity modeling demonstrated a relationship between relative permeability in the rock matrix, the influence of relative permeability on rate of change of vapor phase saturation in the matrix, and the influence of vapor phase saturation changes on observed gravity changes. Gravity therefore provided independent validation of the time rate of change in matrix saturations computed in reservoir simulation.

Prediction of matrix dryout using gravity modeling to validate time rate of change in vapor saturations, determined by reservoir simulation, can be an important predictive tool in assessing the limits to sustainable levelized deliverability. As parts of the reservoir reach irreducible liquid saturation the production wells in that area become deprived of a local source of mass transport. Local deprivation precipitates a change in the depletion process of the system as the wells try to make up the local deficit by drainage for more distant sources; if constant mass withdrawal is imposed on that area by make up well drilling, then Darcy's law dictates greater decline in reservoir pressure throughout the area, which in turn translates into accelerated decline in deliverability of all wells in the area. Thereafter the incremental contributions of new make up wells in the affected area will not keep up with the accelerated decline in total area deliverability; a limiting condition for sustainable deliverability from that area has then been reached. This study indicates that such a condition will be reached in the EMID enthalpy group, the major steam supply source (Table. 2), by the year 2000.

Acknowledgements. The simulation technology used in this work is marketed under the brand name TETRAD/ASTRO. Special recognition is due Mr. Larry Murray, Geothermal Division, Unocal Corporation for his patient instruction on the use of ASTRO technology. Thanks to Unocal Corporation management for permission to publish. Most credit goes to the engineers and geoscientists at PGI, Manila, for their professional accountability.

REFERENCES

Atkinson, P.G. and Pedersen, J.R.,(1988), Using precision gravity data in geothermal reservoir engineering modeling studies. Proceedings of the 13th Workshop on Geothermal Reservoir Engineering: Stanford University, Stanford, California, U.S.A.

Benavidez, P. J., Mosby, M. D., Leong, J. K., and Navarro, V. C. (1988) Development and Performance of the Bulalo Geothermal Field. Proceedings of the 10th New Zealand Geothermal Workshop, Aukland, New Zealand.

Grant, M. A., Donaldson, I. G, and Bixley, P. F. (1982) *Geothermal Reservoir Engineering*. Academic Press, Inc., New York, N.Y.

San Andres, R. B. and Pedersen, J. R. (1992), Monitoring the Bulalo Geothermal Reservoir Using Precision Gravity Data. Manuscript submitted for publication in *Geothermics Special Issue: Geothermal Systems of the Philippines*.

Villadolid, F. L. (1991) The Application of Natural Tracers in Geothermal Development: The Bulalo, Philippines Experience. Proceedings of the 13th New Zealand Geothermal Workshop, Auckland, New Zealand, pp. 69-74.